

 Open access • Journal Article • DOI:10.1089/TEN.2005.11.357

Differentiation ability of rat postnatal dental pulp cells in vitro. — [Source link](#)





[Weibo Zhang](#), [X.F. Walboomers](#), [Joop G.C. Wolke](#), [Zhuan Bian](#) ...+2 more authors

Published on: 03 May 2005 - [Tissue Engineering](#) (Mary Ann Liebert, Inc. 2 Madison Avenue Larchmont, NY 10538 USA)

Topics: [Dentin sialophosphoprotein](#), [Stem cell](#), [Stem cell marker](#), [Progenitor cell](#) and [Alkaline phosphatase](#)

Related papers:

- [Postnatal human dental pulp stem cells \(DPSCs\) in vitro and in vivo](#)
- [Stem Cell Properties of Human Dental Pulp Stem Cells](#)
- [SHED: Stem cells from human exfoliated deciduous teeth](#)
- [The performance of human dental pulp stem cells on different three-dimensional scaffold materials.](#)
- [Dentin Regeneration by Dental Pulp Stem Cell Therapy with Recombinant Human Bone Morphogenetic Protein 2](#)

Share this paper:    

View more about this paper here: <https://typeset.io/papers/differentiation-ability-of-rat-postnatal-dental-pulp-cells-4e2h1vxggx>

PDF hosted at the Radboud Repository of the Radboud University Nijmegen

The following full text is a publisher's version.

For additional information about this publication click this link.

<http://hdl.handle.net/2066/49052>

Please be advised that this information was generated on 2022-05-31 and may be subject to change.

Osteochondral repair in the rabbit model utilizing bilayered, degradable oligo(poly(ethylene glycol) fumarate) hydrogel scaffolds

Theresa A. Holland,¹ Esther W. H. Bodde,² L. Scott Baggett,³ Yasuhiko Tabata,⁴ Antonios G. Mikos,¹ John A. Jansen²

¹Department of Bioengineering, Rice University, P.O. Box 1892, MS 142, Houston, Texas 77251-1892

²Department of Periodontology and Biomaterials, University Medical Center, THK 117, University of Nijmegen, P.O. Box 9101, 6500 HB Nijmegen, The Netherlands

³Department of Statistics, Rice University, P.O. Box 1892, MS 138, Houston, Texas 77251-1892

⁴Department of Biomaterials, Field of Tissue Engineering, Institute for Frontier Medical Sciences, Kyoto University, 53 Kawara-cho Shogoin, Sakyo-ku, Kyoto 606-8507, Japan

Received 29 November 2004; revised 25 February 2005; accepted 2 March 2005

Published online 28 July 2005 in Wiley InterScience (www.interscience.wiley.com). DOI: 10.1002/jbm.a.30379

Abstract: In this study, hydrogel scaffolds, based on the polymer oligo(poly(ethylene glycol) fumarate) (OPF), were implanted into osteochondral defects in the rabbit model. Scaffolds consisted of two layers—a bottom, bone forming layer and a top, cartilage forming layer. Three scaffold formulations were implanted to assess how material composition and transforming growth factor- β 1 (TGF- β 1) loading affected osteochondral repair. Critical histological evaluation and scoring of the quantity and quality of tissue in the chondral and subchondral regions of defects was performed at 4 and 14 weeks. At both time points, no evidence of prolonged inflammation was observed, and healthy tissue was seen to infiltrate the defect area. The quality of this tissue improved over time with hyaline cartilage filling the chondral region and a mixture of trabecular and compact bone filling the subchondral region at 14 weeks. A promising degree of Safranin O staining and chondrocyte organi-

zation was observed in the newly formed surface tissue, while the underlying subchondral bone was completely integrated with the surrounding bone at 14 weeks. Material composition within the bottom, bone-forming layer did not appear to affect the rate of scaffold degradation or tissue filling. However, no bone upgrowth into the chondral region was observed with any scaffold formulation. TGF- β 1 loading in the top layer of scaffolds appeared to exert some therapeutic affect on tissue quality, but further studies are necessary for scaffold optimization. Yet, the excellent tissue filling and integration resulting from osteochondral implantation of these OPF-based scaffolds demonstrates their potential in cartilage repair strategies. © 2005 Wiley Periodicals, Inc. *J Biomed Mater Res* 75A: 156–167, 2005

Key words: articular cartilage engineering; degradable hydrogel; gelatin microparticles; *in vivo* osteochondral defect

INTRODUCTION

Chronic joint pain and arthritis affects approximately one-third of adults in the United States,¹ and is the leading causes of disabilities among Americans.² Many of these individuals suffer from lesions to articular cartilage, the thin tissue lining diarthrodial joints that dissipates compressive loads and allows for pain-free movement.³ Lesions, commonly inflicted during

improper joint loading, sudden joint rotation, or direct impact to a joint, often fail to heal properly due to the complex structure of this unique tissue.^{3,4} In particular, articular cartilage is an avascular tissue with a relatively sparse cell population and a dense, well-ordered extracellular matrix.^{5,6} Because articular cartilage exhibits limited intrinsic repair, lesions may lead to further joint degeneration and the onset of osteoarthritis.^{4,7,8}

Treatment options for patients with articular cartilage lesions are currently restricted to surgical procedures aimed at either stimulating a healing response at the injury site or filling the lesion with a tissue graft.^{7,9} The former strategy is undertaken by invasive drilling to deepen cartilage lesions to access the bioactive molecules and reparative cells in the underlying bone marrow. The strategy of tissue grafting requires surgical disruption of healthy tissue to harvest a

Correspondence to: J. A. Jansen; e-mail: jjansen@dent.umcn.nl

Contract grant sponsor: the National Institutes of Health; contract grant number: R01 AR48756 (to A.G.M.)

Contact grant sponsor: Whitaker Foundation Graduate Fellowship (to T.A.H.)

TABLE I
Material Composition and TGF- β 1 Loading in the Upper and Lower Layers of the Three Formulations of OPF Scaffolds Implanted into Osteochondral Defects

	Scaffold Formulations		
	C ⁺ /C	C ⁺ /H	C ⁻ /H
Chondral layer	Composite: Gel encapsulating TGF- β 1-loaded microparticles	Composite: Gel encapsulating TGF- β 1-loaded microparticles	Composite: Gel encapsulating blank microparticles
Subchondral layer	Composite: Gel encapsulating blank microparticles	Hydrogel with no microparticles or TGF- β 1	Hydrogel with no microparticles or TGF- β 1

source of cartilage, periosteal, or perichondrial cells for subsequent transplantation at the lesion site. Thus, both treatment options inflict further tissue destruction before any therapeutic effect can be achieved. Additionally, both surgical strategies have demonstrated very limited long-term efficacy. In general, surgical abrasion or drilling appears to produce mainly fibrocartilage or fibrous tissue at the repair site, which often deteriorates over time.^{5,9,10} Graft delamination and endochondral ossification are frequently encountered following tissue transplantation.⁹⁻¹¹ Accordingly, new treatment options are necessary for the treatment of articular cartilage defects.

Through a series of investigations, our laboratory has developed a novel class of injectable materials for the delivery of bioactive molecules to cartilage lesions to enhance tissue repair.¹²⁻¹⁴ These systems are based on oligo(poly(ethylene glycol) fumarate) (OPF), a synthetic polymer that can be used to fabricate biodegradable and biocompatible hydrogels.^{15,16} OPF, a water soluble polymer, can be injected into a defect site and crosslinked *in situ* at physiological conditions, thereby eliminating the need for harsh surgeries. Gelatin microparticles, incorporated into these gels at the time of crosslinking, have been shown to act as enzymatically digestible porogens to speed scaffold degradation.¹⁴ Sustained growth factor delivery has been achieved by first loading these microparticles with the desired growth factor and then encapsulating the microparticles within the OPF network.¹²⁻¹⁴

This current work evaluates three different formulations of bilayered OPF hydrogel scaffolds in osteochondral repair. A bilayered scaffold design (Table I) was employed to spatially control drug loading and scaffold degradability in the approximate regions where cartilage and bone are found in healthy joints. For all formulations, the upper scaffold layer consisted of an OPF hydrogel in which 0.20 g gelatin microparticles per gram polymer were encapsulated. This scaffold composition was utilized because microparticles embedded in the OPF network at this concentration have previously been shown to act as digestible porogens.¹⁴ Accordingly, it was hypothesized that this composition would allow for rapid and adequate cell infiltration to the chondral portion of defects from the surrounding cartilage and synovium.¹⁷

In two scaffold formulations (abbreviated as C⁺/C and C⁺/H), microparticles within this upper composite layer were loaded with transforming growth factor- β 1 (TGF- β 1), while microparticles in the third scaffold formulation (abbreviated as C⁻/H) were loaded with PBS. TGF- β 1 is an excellent candidate for cartilage drug delivery strategies as this growth factor has been shown to enhance chondrocyte proliferation^{18,19} to promote the chondrogenic differentiation of progenitor cells,²⁰⁻²² and to increase cartilage extracellular matrix synthesis.²³⁻²⁵ The bottom layer of all scaffolds was unloaded (TGF- β 1-free) because TGF- β 1 delivery to the osseous tissue of osteochondral defects has resulted in bone upgrowth into the cartilaginous region of defects.²⁶ In two scaffold formulations (C⁺/H and C⁻/H), the bottom layer was composed solely of an OPF hydrogel without any porogen. This material composition was chosen to act as a structural barrier to further prevent bone upgrowth, because OPF hydrogels have been shown to degrade slower than OPF-gelatin microparticle composite gels.¹⁴

Histological evaluation of the quantity and quality of tissue repair in the upper and lower portion of defects treated with these three scaffold formulations was performed at both 4 and 14 weeks to assess the following questions:

1. Do these novel, hydrogel scaffolds support cartilage and bone growth in the rabbit osteochondral defect model?
2. How does the quality and quantity of tissue repair compare over time?
3. Does the rate of material degradation in the lower, bone forming portion of scaffolds affect tissue formation?
4. How does TGF- β 1 delivery to the upper portion of osteochondral defects affect cartilage repair?

EXPERIMENTAL METHODS

Gelatin microparticle fabrication and loading

Gelatin microparticles were fabricated from acidic gelatin (Nitta Gelatin Inc., Osaka, Japan) and crosslinked in

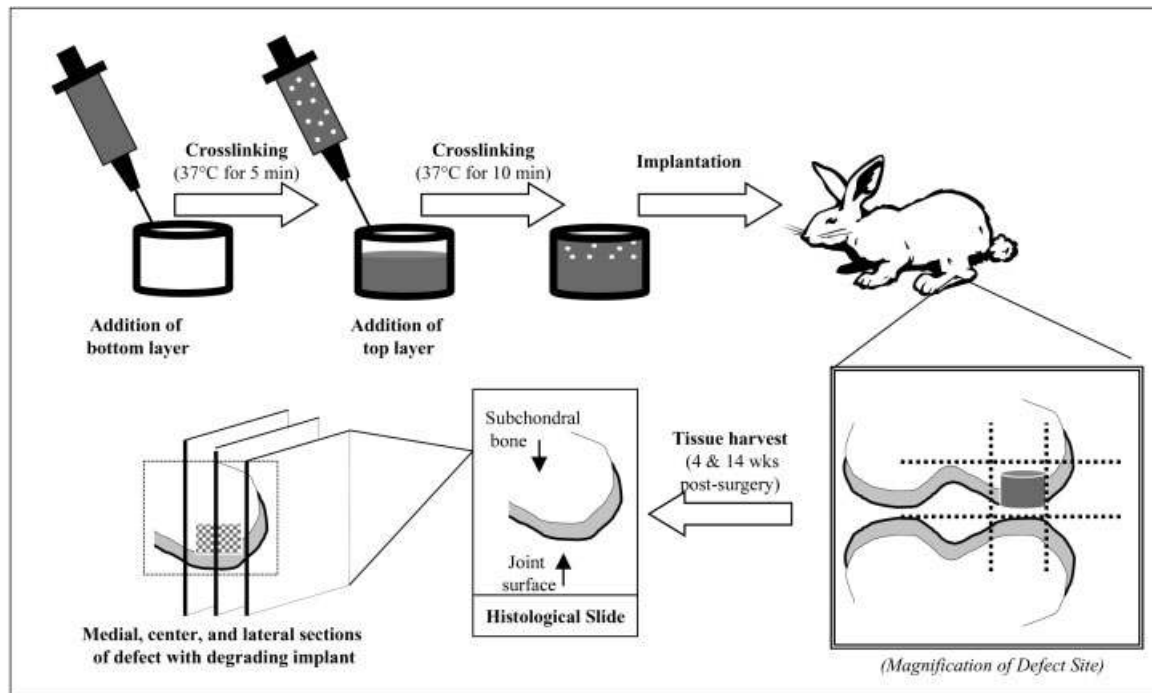


Figure 1. Overview of the methods utilized for scaffold fabrication and implantation, as well as subsequent retrieval and processing of tissue.

10 mM glutaraldehyde (Sigma, St. Louis, MO) according to previously established methods.²⁷ After drying, the microparticles were sieved to obtain particles 50–100 μm in size and then sterilized by exposure to ethylene oxide gas.²⁸

Sterile microparticles were then loaded with TGF- β 1 by swelling in an aqueous solution of TGF- β 1 at pH 7.4 according to previous methods.^{13,14} At this pH, TGF- β 1 (with an isoelectric point of 9.5) is positively charged, and therefore, forms a polyionic complexation with negatively charged acidic gelatin (isoelectric point of 5.0).^{27,28} A TGF- β 1 loading solution concentration of 1.2 μg TGF- β 1/mL PBS was utilized to achieve an overall growth factor loading of approximately 200 ng TGF- β 1/mL in the top crosslinked, layer of scaffolds. This concentration of TGF- β 1 has previously been shown to be therapeutic in the treatment of full and partial thickness rabbit and porcine defects.^{26,29} Blank microparticles were loaded with PBS in a similar fashion.

OPF synthesis

OPF with an initial number average molecular weight of $12,300 \pm 100$ and weight average molecular weight of $51,300 \pm 6,700$ was synthesized according to a method developed in our laboratory.³⁰ Molecular weight determination was likewise conducted using established procedures for gel permeation chromatography with samples run in triplicate.¹⁴ The resulting OPF was sterilized by exposure to UV light for 3 h following an established technique.³¹

Scaffold fabrication

Table I displays the three different scaffold formulations fabricated for this study. All scaffolds consisted of two layers: a top cartilage-forming layer, and a bottom bone-forming layer with respective thicknesses of 1 and 2 mm. Although the thickness of articular cartilage was expected to vary among animals, these dimensions were chosen as a means of tailoring scaffold composition and drug loading to the upper or lower portion of defects, rather than as a model of exact anatomy. Because the animals utilized in this study were already undergoing bilateral joint surgery for creation of the osteochondral defects, scaffolds were implanted, rather than injected, at the defect site.

As noted in Table I, the scaffold formulations have been assigned abbreviations based on the material compositions within each layer—either an OPF hydrogel layer (H) or a composite gel layer (C) in which gelatin microparticles were encapsulated in the OPF network. The first letter of each abbreviation corresponds to the material composition of the upper, cartilage-forming layer. Subscripts “–” or “+” respectively refer to upper layers containing microparticles loaded with PBS or loaded with TGF- β 1. No growth factors were added to the bottom bone-forming layer of any scaffold formulation.

All scaffolds were fabricated using a two-step crosslinking procedure (Fig. 1) in which an OPF solution with the desired bottom layer composition was first injected into a mold and partially crosslinked prior to the injection and crosslinking of the upper layer. More specifically, 0.15 g OPF was dissolved in 395 μl of PBS containing 14 mg *N,N'*-methylene bisacrylamide (Sigma, St. Louis, MO) as a crosslinking

agent. Then, the appropriate amount of microparticles (32 or 0 mg) was added to the polymer solution with an additional 118 μL PBS. The resulting mixture was thoroughly vortexed. Finally, 51 μL of 0.3 M tetramethylethylenediamine (in PBS) (Sigma, St. Louis, MO) and 51 μL of 0.3 M ammonium persulfate (in PBS; Sigma, St. Louis, MO) were added to initiate crosslinking. After vortexing, the suspension was injected into a cylindrical Teflon mold (3 mm in diameter) to a height of 2 mm and incubated at 37°C to achieve crosslinking. The cytocompatibility of this tetramethylethylenediamine/ammonium persulfate initiating system has previously been demonstrated by the successful encapsulation of rat marrow stromal cells in OPF hydrogels during the time of crosslinking.^{31,32}

After 5-min incubation, this formulation of OPF forms a partially crosslinked hydrogel, enabling lamination to a second layer.^{14,33} Accordingly, at this time, a second solution of OPF–gelatin microparticles was injected into the Teflon mold to form the upper scaffold layer (1 mm in height). Prior to injection, this solution was mixed as previously described. The mold was then incubated at 37°C for 10 min to achieve complete crosslinking of both layers. It should be noted that all PBS, initiator, and bisacrylamide solutions were sterilized prior to use by filtration through a cellulose acetate membrane filter (0.2 μm pore diameter) according to an established procedure.³¹ The final dimensions of all scaffolds matched the dimensions of osteochondral defects in the rabbit model (3 mm in diameter \times 3 mm in depth).^{34–36} Scaffolds were fabricated 2 to 4 h prior to implantation.

Animal surgery

Seventeen, 4-month-old New Zealand white rabbits were utilized in this study. All surgical procedures followed protocols approved by the University of Nijmegen's Animal Care and Use Committee and were based on a well-established bilateral, rabbit, osteochondral defect model.^{34–36} Eight of the 17 rabbits were used to examine tissue repair at 4 weeks, with the remaining nine rabbits utilized to examine repair at 14 weeks.

Prior to surgery, anesthesia was induced by an intravenous injection of Hypnorm® (0.32 mg/mL fentanyl citrate and 10 mg/mL fluanisone) and atropine. General inhalation anesthesia was then maintained by a mixture of nitrous oxide, isoflurane, and oxygen administered through a constant volume ventilator. To reduce peri-operative infection risk and to minimize postoperative discomfort, antibiotic prophylaxis (Baytril 2.5%, Enrofloxacin, 5–10 mg/kg) and Fynadyne® were preoperatively administered to the rabbits.

After administration of anesthesia, rabbits were immobilized on their back. Hair from both legs of each animal was shaved, and the legs disinfected with povidone–iodine. Both knee joints were then exposed through a medial parapatellar longitudinal incision. The capsule was incised, and the medial femoral condyle exposed after lateral luxation of the patella. With the knee maximally flexed, a full-thickness defect (3 mm in diameter and 3 mm in depth) was created in the center of the condyle using a dental drill (KAVO, Intra-sept 905, KAVO Nederland BV, Vianen, The Netherlands). A 2-mm drill bit was first used to establish a 2-mm diameter

defect. This defect was then irrigated and gradually enlarged using drill bits with a diameter of 2.8 mm and then 3.0 mm. All bits were fashioned with a 3 mm stop to ensure a defect of precisely 3 mm in depth was created. All debris was removed from the defect with a curette and the edge carefully cleaned with a scalpel blade.

A scaffold was then placed into the defect. Subsequently, the patella was repositioned, and the capsule and muscle closed with a continuous 4-0 Vicryl suture. Finally, the skin was closed with single intracutaneous 4-0 Vicryl sutures. This procedure was repeated for both knees of each rabbit with different scaffold formulations implanted into the right and left knees of each rabbit. More specifically, five rabbits received one C⁺/H scaffold and one C⁺/C scaffold, while an additional six rabbits received one C⁻/H scaffold and one C⁺/H scaffold. Finally, the last six rabbits received one C⁺/C and one C⁻/H scaffold.

To minimize postoperative discomfort, Fynadyne® was administered for 2 days postoperatively. The animals were housed in conventional rabbit cages that allowed for unrestricted weight-bearing activity and were observed for signs of pain, infection, and proper activity.

Tissue processing

At 4 and 14 weeks postsurgery, rabbits were euthanized by intravenous administration of Nembutal (pentobarbital). The tissue surrounding the medial femoral condyle was retrieved en bloc. Specimens were fixed in 10% buffered formalin (pH 7.4) for 1 week, decalcified in Formical2000 (Decal Corporation, Congers, NY) for 2 weeks, dehydrated through graded ethanols, and embedded in paraffin. Using a microtome (Leica RM 2165, Leica Microsystems, Nussloch, Germany), longitudinal sections of 6 μm in thickness were taken throughout the defect. Sections from the defects' center and lateral and medial edges were then stained with hematoxylin and eosin (H&E). Likewise, center, lateral, and medial sections were separately stained with Safranin O/light green and Masson's trichrome. This methodical processing of the sections allowed for subsequent evaluation of tissue repair at the defect edges and center.

In addition to standard H&E, the two additional staining methods enabled identification of key attributes of the newly formed tissue—in particular, glycoaminoglycan and collagen content. Safranin O is routinely used in cartilage histology because this stain colors basophilic structures, like the negatively charged glycoaminoglycans of articular cartilage, with shades of red. Light green is a neutral stain utilized as a counter stain in Safranin O-stained sections. Masson's trichrome staining is also a well-established histological technique for evaluating connective tissue. This technique identifies collagen fibers with a green color, while cell nuclei and cytoplasm are respectively stained black and red.³⁷

Histological scoring

Histological sections were blindly and independently scored by two evaluators (TH and EB) using a modified

graded system based on the five histological characteristics examined in the original O'Driscoll method for examining tissue graft performance: graft integration and integrity, and cartilage morphology, regularity, and thickness.³⁸ However, because the present study examined the performance of degradable implants, rather than tissue grafts, this system was amended to examine neo-tissue ingrowth and integration, rather than graft integrity and integration (Table II). Additionally, because the material composition of the bottom subchondral layer of these implants was varied to examine how the rate of implant degradation affected tissue formation, parameters were also included to separately examine neo-tissue ingrowth and morphology in this region. Overall implant degradation was also scored.

Finally, following well-established modifications to the original O'Driscoll system, additional parameters examined potential chondrocyte clustering within the newly formed cartilaginous tissue,^{39–41} as well as the cellularity and GAG content (assessed by Safranin O staining) within the neo-tissue and in the cartilage immediately adjacent to the defect.^{36,39,41} Similarly, apparent total collagen content in the neo-tissue was assessed by Masson's trichrome staining. These parameters were scored relative to the respective characteristics of uninjured cartilage far removed from the defect site. Thus, the histological scoring system shown in Table II facilitated a thorough, systematic means of evaluating tissue quality and quantity in the overall 3 × 3 mm defect, as well as in the subchondral (the bottom 2 mm) and chondral (the upper 1 mm) regions of defects. Furthermore, this comprehensive system allowed for assessment of possible degenerative changes in the tissue adjacent to defects.

Statistical analysis

Ordered logistic regression of histological scores was performed using SAS Version 8.2 statistical software (SAS, Cary, NC). This statistical method provides a means of assessing potential factors affecting outcomes with discrete, ordinal values.⁴² For each histological parameter, ordered logistic regression was performed to analyze the potential single factor affects of time, scaffold formulation, and location within the defect (edge vs center sections). The Wald chi-square test statistic with a significance level of 0.05 was first used to confirm the validity of each regression. An analysis of effects was then performed with a significance level of 0.05. Potential two and three factor interactions amongst time, scaffold formulation, and location were also evaluated for each histological parameter.

Calculation of average histological scores

Ordered logistic regression revealed that section location (edge vs center) within defects was not a significant factor affecting any of the 12 histological parameters. Thus, for each parameter, the medial, lateral, and center scores for a particular defect were averaged. Then, at each time point, the mean score and corresponding standard deviation amongst these averages was calculated for each treatment

TABLE II
Histological Scoring System for Evaluation of Overall Tissue Filling (a), Subchondral Bone Repair (b), and Cartilage Repair (c) in Rabbit, Osteochondral Defects

(a) Overall defect evaluation (throughout the entire defect depth)	Score
1. Percent filling with neo-formed tissue	
100%	3
>50%	2
<50%	1
0%	0
2. Percent degradation of the implant	
100%	3
>50%	2
<50%	1
0%	0
(b) Subchondral bone evaluation (within the bottom 2 mm of defect)	Score
3. Percent filling with neo-formed tissue	
100%	3
>50%	2
<50%	1
0%	0
4. Subchondral bone morphology	
Normal, trabecular bone	4
Trabecular, with some compact bone	3
Compact bone	2
Compact bone and fibrous tissue	1
Only fibrous tissue or no tissue	0
5. Extent of neo-tissue bonding with adjacent bone	
Complete on both edges	3
Complete on one edge	2
Partial on both edges	1
Without continuity on either edge	0
(c) Cartilage evaluation (within the upper 1 mm of defect)	Score
6. Morphology of neo-formed surface tissue	
Exclusively articular cartilage	4
Mainly hyaline cartilage	3
Fibrocartilage	2
Only fibrous tissue or bone	1
No tissue	0
7. Thickness of neo-formed cartilage	
Greater than surrounding cartilage	3
Similar to the surrounding cartilage	2
Less than the surrounding cartilage	1
No cartilage	0
8. Joint surface regularity	
Smooth, intact surface	3
Surface fissures (<25% neo-surface thickness)	2
Deep fissures (25–99% neo-surface thickness)	1
Complete disruption of the neo-surface	0
9. Chondrocyte clustering	
None at all	3
<25% chondrocytes	2
25–100% chondrocytes	1
No chondrocytes present (no cartilage)	0
10. Cell and glycoaminoglycan (GAG) content of neo-formed cartilage	
Normal cellularity with normal Safranin O staining	3
Normal cellularity with moderate Safranin O staining	2
Clearly less cells with poor Safranin O staining	1
Few cells with no or little Safranin O staining or no cartilage	0
11. Collagen content	
Normal	3
Moderately reduced	2
Severely reduced	1
Absent or no cartilage	0
12. Cell and glycoaminoglycan (GAG) content of adjacent cartilage	
Normal cellularity with normal GAG content	3
Normal cellularity with moderate GAG content	2
Clearly less cells with poor GAG content	1
Few cells with no or little GAGs or no cartilage	0

group. These values are reported in Tables III and IV as mean scores per formulation (MSF) \pm standard deviation.

It should be noted that for all parameters, except parameter 7, scores of maximum value correspond to the characteristics of healthy, uninjured tissue. For parameter 7 (neo-cartilage thickness), a score of 2, rather than the maximum value of 3, corresponds to normal cartilage thickness. Although neo-cartilage thickness was commonly observed to be thinner than the surrounding cartilage, only one instance of overfilling was noted. Thus, average scores for this parameter accurately represent relative tissue thickness.

RESULTS

Animal health and macroscopic joint appearance at recovery

Animals appeared to recover quickly from the bilateral surgical procedure and were observed to regain full movement within less than 1 week. The rabbits continued to exhibit no physical limitations, with normal behavior and movement observed throughout the 14-week period. It should be noted that complications during the surgical creation of one defect led to exclusion of that specimen from the study. With all other defects, no signs of inflammation, infection, or swelling were noticed upon visible inspection of the joint surfaces at the time of tissue retrieval.

Histological appearance

Tissue repair at 4 weeks

No evidence of a persistent inflammatory response was observed at 4 weeks despite the significant extent of implant degradation that was observed at this early time point. Immature tissue was seen to fill greater than 50% of the defect area in histological sections of joints treated with all scaffold formulations. The overall percentage of tissue filling and scaffold degradation appeared to vary among all defects, regardless of scaffold type. Compact bone and a small amount of fibrous tissue generally filled the subchondral portion of defects (the bottom 2 mm). However, in many specimens, especially those with little scaffold material remaining, some trabecular bone was already present at this early time point. Overall, this osseous tissue was well integrated with the surrounding bone.

Likewise, the newly formed tissue in the chondral region of defects (the upper 1 mm) displayed continuity with both the adjacent cartilage and underlying subchondral tissue. This neo-surface had the appearance of fibrocartilage or fibrous tissue and was gener-

ally thinner than the surrounding, uninjured cartilage. Elongated, thin cells and sparse Safranin O staining were observed at 4 weeks (Fig. 2). Some fissures in the neo-surface were present, but these generally did not extend to the underlying bone. Both the subchondral and chondral tissue adjacent to the defect site maintained a healthy appearance.

Tissue repair at 14 weeks

In general, by 14 weeks, defects were completely filled with tissue, and scaffolds were completely degraded. With all treatment groups, the neo-formed subchondral and chondral tissue had undergone considerable remodeling between 4 and 14 weeks, as apparent in the morphology of the newly formed tissue at this later time point (Fig. 3). In some sections, the only visible marker of the former defect area was a slightly thinner cartilage layer with less intense Safranin O staining than the surrounding joint surface. Trabecular bone, and sometimes a small amount of remaining compact bone, filled the subchondral region. In all cases, this bone was completely integrated with the adjacent bone.

The new joint surface was also well-integrated with the surrounding cartilage at 14 weeks, but was occasionally dotted with fissures as shown in Figure 3(i). With all treatment groups, chondrocytes now populated the former defect area but were reduced in number when compared to the uninjured cartilage. These chondrocytes were often arranged in a zonal organization resembling healthy articular cartilage. As shown in the magnifications of Figures 3(g) and 3(h), chondrocytes near the joint surface were slightly elongated. Below these cells, more rounded chondrocytes were seen to form columns and to stain more intensely for GAG, as expected for cells in the intermediate zone of articular cartilage.^{3,43} Cartilage surrounding this neo-formed surface maintained a healthy appearance and thickness [Fig. 3(a-c)].

Histological scoring

Overall analysis

A general improvement among histological scores for all treatment groups was observed between 4 and 14 weeks. In fact, statistical evaluation of scores revealed that time was a significant factor affecting tissue and bone filling, bone and cartilage morphology, cartilage thickness, and chondrocyte clustering, as well as cell, GAG, and collagen content (parameters 1, 3-4, 6-7, and 9-12). Section location (edge vs center of the defect) was not seen to be a significant factor for

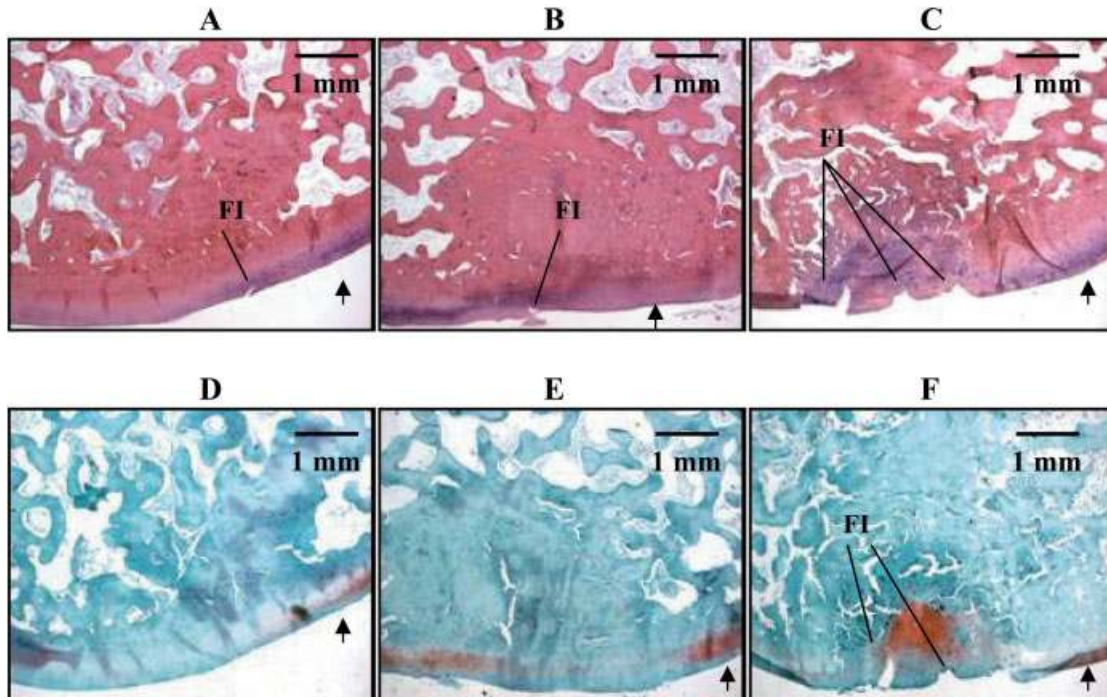


Figure 2. Sections showing representative 4-week tissue repair in three defects after osteochondral implantation of C^+ / C (A and D), C^+ / H (B and E), and C^- / H (C and F) scaffolds. (A–C) H&E-stained tissue sections; (D–F) sections stained with Safranin O/light green. Original magnification of all sections is $2.5\times$. Arrows point towards the joint surface, while surface fissures are respectively indicated by FI. [Color figure can be viewed in the online issue, which is available at www.interscience.wiley.com.]

any of the 12 histological scores at either time point. Contrary to expectations, scaffold type (C^+ / C , C^+ / H , or C^- / H) was only found to be a significant factor affecting one of the histological markers—in particular, joint surface regularity. Additional analysis revealed that no two or three factor interactions were present among time, location, and scaffold type.

Histological scores at 4 weeks

As previously discussed, some variability in tissue filling and scaffold degradation was observed in 4 week sections. Again, scaffold type was not seen to influence the degree of tissue filling or scaffold degradation. Mean histological scores for subchondral bone morphology were between 2.0 and 1.0 (Table III), indicating the predominance of remodeling compact bone with some remaining fibrous tissue in this portion of defects at 4 weeks. Contrary to expectations, the material composition of the bottom layer of scaffolds did not influence bone filling, morphology, or integration. However, no bone upgrowth into the chondral region was observed with any of the treatment groups.

Histological evaluation revealed that TGF- β 1 delivery had little effect on early cartilage repair. Regardless of treatment group, the neo-surface at 4 weeks

scored between 1.0 and 2.0 for surface tissue morphology, reflecting the fibrous nature of this new surface. Critical histological scoring revealed that this tissue was thinner and contained lower cell, GAG, and collagen content than the surrounding uninjured cartilage (see Table III). Very limited degenerative changes were observed in the cartilage adjacent to defects. As shown in Table III, mean scores for cell and GAG content in the surrounding cartilage tissue (parameter 12) were at or near 2.0 for all formulations, indicating normal cellularity with moderately reduced GAG content. Again, these findings further confirm the biocompatibility of these OPF composites and their degradation products. By 14 weeks, the surrounding cartilage, as well as the neo-formed surface, displayed overall improvements in tissue quality as reflected in the higher histological scores at this later time point.

Histological scores at 14 weeks

In general, scaffolds were completely degraded at 14 week. Tissue filling was seen to statistically improve by 14 weeks. However, perhaps the most striking improvements between 4 and 14 weeks were observed in the morphology of both the subchondral and chondral regions of the former defect areas. Although the 4-week mean scores for subchondral bone mor-

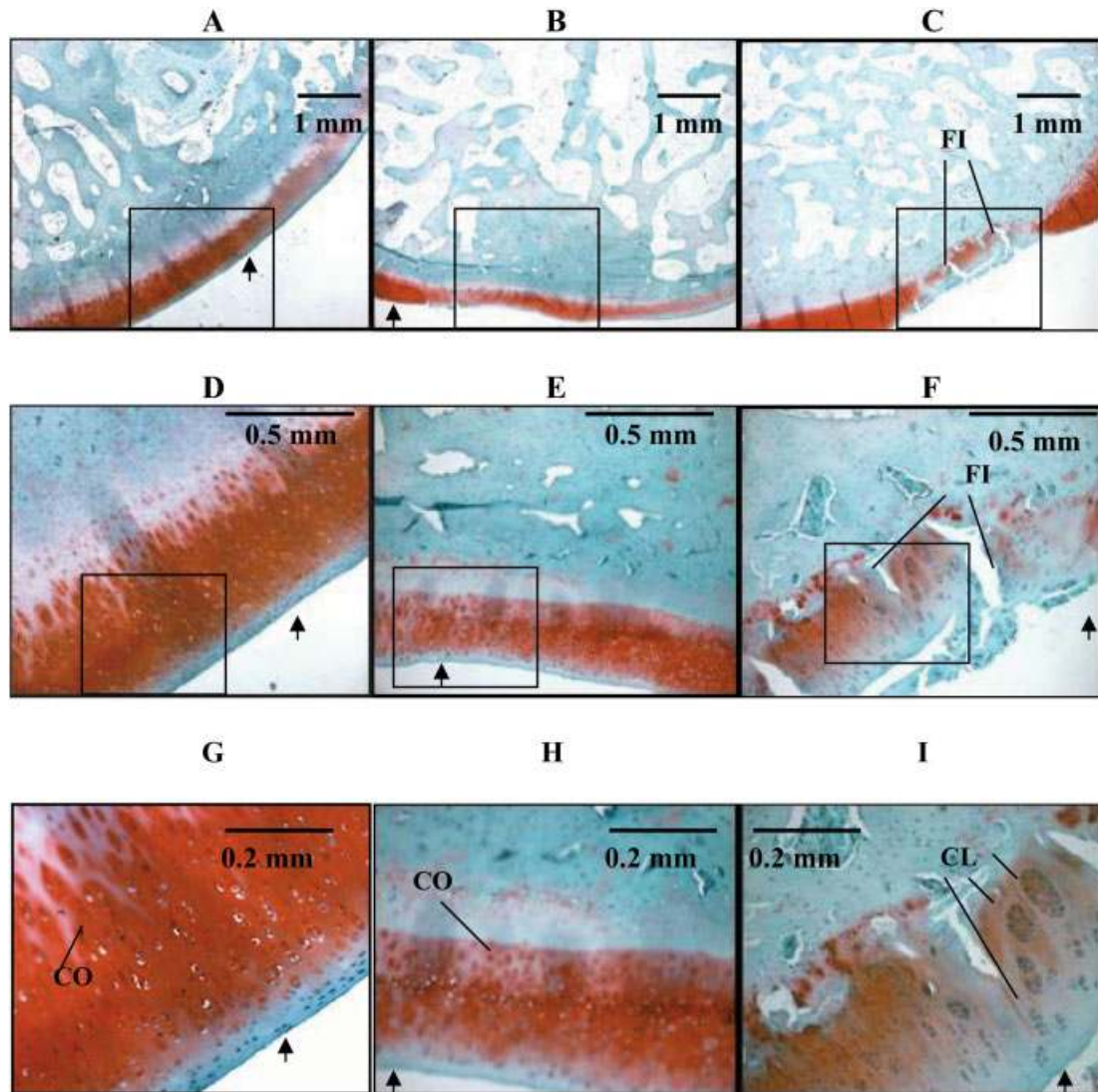


Figure 3. Sections (stained with Safranin O/light green) showing representative 14-week tissue repair in three defects after osteochondral implantation of C^+ /C (A, D, and G), C^+ /H (B, E, and H), and C^- /H (C, F, and I) scaffolds. The boxed regions in (A–C) (2.5 \times magnification) are shown at higher magnifications in (D–F) (10 \times), and (G–I) (20 \times). Arrows point towards the joint surface, while columnar arrangements of chondrocytes, cell clusters, and cartilage fissures are respectively indicated by CO, CL, and FI. [Color figure can be viewed in the online issue, which is available at www.interscience.wiley.com.]

phology were below 2.0 for all treatments, by 14 weeks these scores had risen to 3.0 ± 0.7 , 2.7 ± 0.6 , 3.1 ± 0.9 , for defects treated with C^+ /C , C^+ /H , and C^- /H , respectively. Thus, the compact bone and fibrous tissue present at 4 weeks underwent remodeling to form trabecular bone at 14 weeks. As shown in Figure 3, this bone was completely integrated with the surrounding bone. In fact, maximum scores of 3.0, indicating complete bonding on both defect edges, were awarded to all tissue sections evaluated at 14 weeks.

Tissue quality in the chondral portion of the former defect area had also improved considerably by week 14 (see Fig. 3). In fact, scores for tissue morphology, thickness, chondrocyte clustering, and cell, GAG, and collagen content were statistically higher at 14 weeks

than at 4 weeks. For example, scores for cell and GAG content, which had been at or below 1.0 at 4 weeks, now approached 2.0 at 14 weeks, indicating an increase in both cellularity and GAG content. Likewise, scores for total collagen content were also seen to improve between 4 and 14 weeks. Perhaps most indicative of the overall improvement in tissue quality were the elevated 14 week mean scores for surface tissue morphology (2.9 ± 0.6 , 2.7 ± 0.5 , 2.6 ± 0.8 for C^+ /C , C^+ /H , and C^- /H treatment groups, respectively). These scores reflected the high frequency of hyaline cartilage filling the chondral region and the zonal arrangement of chondrocytes at 14 weeks. It should be noted that this cartilage was still thinner than the surrounding cartilage, but its thickness had statistically improved between 4 and 14 weeks. Al-

TABLE III
Mean Histological Scores per Scaffold Formulation (MSF) at 4 Weeks Postsurgery

Histological Parameter	Mean Score per Formulation		
	C ⁺ /C (n = 4)	C ⁺ /H (n = 6)	C ⁻ /H (n = 5)
<i>Overall defect evaluation</i>			
1. Percent filling with neo-formed tissue	2.2 ± 0.8	2.7 ± 0.4	2.3 ± 0.7
2. Percent degradation of the implant	2.7 ± 0.5	2.7 ± 0.4	2.3 ± 0.7
<i>Subchondral bone evaluation</i>			
3. Percent filling with neo-formed tissue	2.0 ± 0.7	2.1 ± 1.1	2.1 ± 0.8
4. Subchondral bone morphology	1.5 ± 1.1	1.5 ± 1.0	1.7 ± 0.7
5. Extent of neo-tissue bonding with adjacent bone	2.0 ± 1.0	2.1 ± 1.3	3.0 ± 0.0
<i>Cartilage evaluation</i>			
6. Morphology of neo-formed surface tissue	1.8 ± 0.6	1.6 ± 0.5	1.6 ± 0.5
7. Thickness of neo-formed cartilage	1.3 ± 1.0	0.7 ± 0.4	0.8 ± 0.8
8. Joint surface regularity	2.6 ± 0.5	2.0 ± 0.6	1.7 ± 0.8
9. Chondrocyte clustering	1.6 ± 1.1	1.2 ± 1.0	0.9 ± 0.9
10. Cell and GAG content of neo-formed cartilage	1.1 ± 0.8	0.7 ± 0.8	0.8 ± 0.8
11. Collagen content	1.7 ± 1.2	1.2 ± 0.9	1.3 ± 1.3
12. Cell and GAG content of adjacent cartilage	2.3 ± 0.3	1.8 ± 0.3	2.6 ± 0.4

Values are shown as mean ± standard deviation.

though Safranin O staining in cartilage immediately adjacent to the former defect was slightly reduced (when compared to cartilage far from the defect site), normal chondrocyte density and arrangement perpetuated this tissue, indicating that no severe, adverse effects were inflicted by these OPF-based scaffolds.

DISCUSSION

The rigorous histological analysis undertaken in this study allowed for critical evaluation of tissue repair in osteochondral defects treated with three different formulations of OPF hydrogel scaffolds. More specifically, the 12-parameter system shown in Table II permitted individual assessment of the neo-formed tissue in both the subchondral and chondral regions of defects. At either time point and in either region of the defect, no evidence of persistent inflammation was observed. Overall, at 4 weeks, scaffolds were largely degraded with immature tissue-filling defects. Although mainly compact bone with some fibrous tissue filled the subchondral region at 4 weeks, this tissue had been remodeled to contain predominantly trabecular bone at 14 weeks. Likewise, the fibrocartilage filling the subchondral region of defects at 4 weeks had been remodeled to contain mainly hyaline cartilage at 14 weeks.

This observed improvement in bone and cartilage morphology indicate the biocompatibility of these OPF-based scaffolds and their degradation products. In previous *in vitro* studies, designed to model the low pH environment typical of prolonged inflammation, OPF-gelatin microparticle composites and OPF hydrogels were seen to degrade at a relatively slow rate at

decreased pH. In fact, less than 60% polymer loss was observed at pH 4.0 after 4 weeks.¹⁴ In the present study, scaffold degradation *in vivo* generally exceeded 60% at 4 weeks. Thus, this observation indicates that low pH, and thus an inflammatory environment, did not persist around the defect site. Furthermore, because neither inflammatory cells nor joint swelling were observed at either 4 or 14 weeks, the biocompatibility of the byproducts from these degrading OPF scaffolds is clearly confirmed.

In this study, the observed rate of implant degradation conformed to the expected degradation kinetics for scaffold layers consisting of an OPF-gelatin microparticle composite at normal, physiological conditions.¹⁴ However, layers containing OPF gels with no microparticles were expected to degrade at a slower rate, as complete degradation at pH 7.4 within 4 weeks was not observed in prior *in vitro* studies.¹⁴ Compressive loading during normal, joint movement may explain this enhanced rate of gel degradation. Scaffold type, and thus composition, did not appear to greatly affect the extent of repair. However, bone upgrowth into the chondral region was not observed with either material composition, demonstrating that both compositions have degradation rates that support controlled osteochondral repair. The similar *in vivo* degradation profiles of these scaffolds may account for the similar healing responses observed among scaffold formulations.

Like scaffold degradation, bone integration was not observed to significantly change between 4 and 14 weeks. Although partial integration was occasionally observed at the early time point, 4 week scores for this parameter were not found to be statistically different from the complete integration observed at 14 weeks.

TABLE IV
Mean Histological Scores per Scaffold Formulation (MSF) at 14 Weeks Postsurgery

Histological Parameter	Mean Score per Formulation		
	C ⁺ /C (n = 4)	C ⁺ /H (n = 6)	C ⁻ /H (n = 5)
<i>Overall defect evaluation</i>			
1. Percent filling with neo-formed tissue*	2.8 ± 0.3	2.6 ± 0.2	2.9 ± 0.2
2. Percent degradation of the implant	2.8 ± 0.3	2.6 ± 0.2	2.9 ± 0.2
<i>Subchondral bone evaluation</i>			
3. Percent filling with neo-formed tissue*	2.8 ± 0.3	2.7 ± 0.3	2.9 ± 0.2
4. Subchondral bone morphology*	3.0 ± 0.7	2.7 ± 0.6	3.1 ± 0.9
5. Extent of neo-tissue bonding with adjacent bone	3.0 ± 0.0	3.0 ± 0.0	3.0 ± 0.0
<i>Cartilage evaluation</i>			
6. Morphology of neo-formed surface tissue*	2.9 ± 0.6	2.7 ± 0.5	2.6 ± 0.8
7. Thickness of neo-formed cartilage*	1.7 ± 0.4	1.7 ± 0.2	1.5 ± 0.6
8. Joint surface regularity	2.6 ± 0.5	2.4 ± 0.4	2.2 ± 0.3
9. Chondrocyte clustering*	2.1 ± 0.7	1.7 ± 0.4	1.9 ± 0.7
10. Cell and GAG content of neo-formed cartilage*	1.9 ± 0.6	1.7 ± 0.5	1.7 ± 0.6
11. Collagen content*	2.3 ± 0.7	2.2 ± 0.6	2.4 ± 1.0
12. Cell and GAG content of adjacent cartilage*	2.8 ± 0.3	2.7 ± 0.3	2.6 ± 0.4

Values are shown as mean ± standard deviation. Asterisks (*) indicate those parameters which were shown to statistically improve over time from 4-week values.

Often, when grafts⁷ or degradable scaffolds^{35,36} are utilized in cartilage repair, incomplete integration with the surrounding tissue is observed upon long-term evaluation. This may lead to displacement of the implant and inflict further joint pain.⁷ Thus, the excellent tissue integration exhibited with these novel scaffolds demonstrates their potential in advancing the treatment of cartilage lesions.

Likewise, the lack of statistical changes in joint surface regularity scores reflects the utility of these scaffolds in cartilage engineering. At both 4 and 14 weeks, disruptions in the joint surface were generally limited to surface fissures, as indicated by the histological scores in Tables III and IV. It should be noted that scaffold type was seen to affect this marker of cartilage repair. In particular, higher scores corresponded with TGF-β1-loaded scaffolds. Although these results suggest some therapeutic effect of the TGF-β1 released from these scaffolds, further research is necessary to investigate why growth factor delivery did not affect additional markers of tissue repair. Because other researchers have also encountered a lack of significant differences between treatment groups upon histological evaluation of osteochondral scaffolds,^{36,44} this issue may be related to the complexity of articular cartilage repair and/or the use of relatively young animals with higher regenerative potential. Although numerous other studies have also utilized the current animal model,^{35,36} future studies will investigate these scaffolds for osteochondral repair in older animals.

However, the excellent tissue filling and integration resulting from osteochondral implantation of these novel OPF-based scaffolds demonstrates their potential for improving cartilage repair. As shown in Figure 3, hyaline cartilage with well-organized chondrocytes

and intense GAG staining was seen to fill the chondral portion of defects at 14 weeks. Trabecular bone with some remodeling compact bone was seen to fill the subchondral region. Untreated rabbit osteochondral defects have been shown to be filled with highly fibrillar, fibrous tissue or fibrocartilage in the chondral region with bone up to or beyond the tidemark.³⁵ Accordingly, the quality of repair achieved with these scaffolds reveals their promise in advancing cartilage repair and compels further *in vivo* investigations with these materials.

CONCLUSIONS

Through osteochondral implantation of OPF-based hydrogels, the potential of this novel class of degradable scaffolds has been demonstrated in the field of cartilage tissue engineering. Specifically, this research illustrates that OPF-based hydrogel scaffolds undergo biocompatible degradation and support healthy tissue growth in rabbit osteochondral defects. Tissue quality was seen to improve over time with mostly hyaline cartilage filling the chondral region and a mixture of trabecular and compact bone filling the subchondral region at 14 weeks. Although scaffold material composition was not seen to affect scaffold degradation or tissue filling, no bone upgrowth into the chondral region was observed, and new bone tissue was completely integrated with the surrounding bone at 14 weeks. Although further studies are necessary to optimize these scaffolds, TGF-β1 loading in the top layer of scaffolds appeared to exert some affect on cartilage quality in the defect area. Accordingly, this research

demonstrates the exciting potential of these OPF-based hydrogels as carriers of bioactive agents for cartilage repair.

The authors acknowledge the expert guidance of Drs. Arnold Caplan and Jizong Gao of Case Western Reserve University with the animal model, and Dr. Pieter Buma, of the University Medical Center Nijmegen with the scoring system.

References

- Bolen J, Helmick C, Sacks J, Langmaid G, Division of Adult and Community Health of National Center for Chronic Disease Prevention and Health Promotion CDC. Prevalence of self-reported arthritis or chronic joint symptoms among adults—United States, 2001. *Mor Mortal Wkly Rep* 2002;51:948–950.
- McNeil J, Binette J, Bureau of the Census, Economics and Statistics Administration of U.S. Department of Commerce, Disability and Health Branch, Division of Birth Defects, Child Development, Disability and Health of National Center for Environmental Health, Health Care and Aging Studies Branch, Division of Adult and Community Health of National Center for Chronic Disease Prevention and Health Promotion CDC. Prevalence of disabilities and associated health conditions among adults—United States, 1999. *Mor Mortal Wkly Rep* 2001;50:120–125.
- LeBaron RG, Athanasiou KA. Ex vivo synthesis of articular cartilage. *Biomaterials* 2000;21:2575–2587.
- Hunziker EB. Articular cartilage repair: Are the intrinsic biological constraints undermining this process insuperable? *Osteoarthr Cartil* 1999;7:15–28.
- Gillogly SD, Voight M, Blackburn T. Treatment of articular cartilage defects of the knee with autologous chondrocyte implantation. *J Orthop Sports Phys Ther* 1998;28:241–251.
- Silver FH, Glasgold AI. Cartilage wound healing. An overview. *Otolaryngol Clin North Am* 1995;28:847–864.
- Minas T. The role of cartilage repair techniques, including chondrocyte transplantation, in focal chondral knee damage. *AAOS Instr Course Lect* 1999;48:629–643.
- Jackson DW, Simon TM. Tissue engineering principles in orthopaedic surgery. *Clin Orthop* 1999;331–345.
- McPherson JM, Tubo R. Articular cartilage injury. In: Lanza RP, Langer R, Vacanti JP, editors. *Principles of tissue engineering*. San Diego, CA: Academic Press; 2000. p 697–709.
- Vangsnest CT Jr, Kurzweil PR, Lieberman JR. Restoring articular cartilage in the knee. *Am J Orthop* 2004;33:29–34.
- Driesang IM, Hunziker EB. Delamination rates of tissue flaps used in articular cartilage repair. *J Orthop Res* 2000;18:909–911.
- Holland TA, Tabata Y, Mikos AG. Dual growth factor delivery from degradable oligo(poly(ethylene glycol) fumarate) hydrogel scaffolds for cartilage tissue engineering. *J Controlled Release* 2005;101:111–125.
- Holland TA, Tabata Y, Mikos AG. In vitro release of transforming growth factor-beta1 from gelatin microparticles encapsulated in biodegradable, injectable oligo(poly(ethylene glycol) fumarate) hydrogels. *J Controlled Release* 2003;91:299–313.
- Holland TA, Tessmar JK, Tabata Y, Mikos AG. Transforming growth factor-beta1 release from oligo(poly(ethylene glycol) fumarate) hydrogels in conditions that model the cartilage wound healing environment. *J Controlled Release* 2004;94:101–114.
- Shin H, Ruhe PQ, Mikos AG, Jansen JA. In vivo bone and soft tissue response to injectable biodegradable oligo(poly(ethylene glycol) fumarate) hydrogels. *Biomaterials* 2003;24:3201–3211.
- Fisher JP, Lalani Z, Bossano CM, Brey EM, Demian N, Johnston CM, Dean D, Jansen JA, Wong ME, Mikos AG. Effect of biomaterial properties on bone healing in a rabbit tooth extraction socket model. *J Biomed Mater Res* 2004;68A:428–438.
- Hunziker EB, Rosenberg LC. Repair of partial-thickness defects in articular cartilage: Cell recruitment from the synovial membrane. *J Bone Joint Surg Am* 1996;78:721–733.
- Rosier RN, O'Keefe RJ, Crabb ID, Puzas JE. Transforming growth factor beta: An autocrine regulator of chondrocytes. *Connect Tissue Res* 1989;20:295–301.
- Vivien D, Galera P, Lebrun E, Loyau G, Pujol JP. Differential effects of transforming growth factor-beta and epidermal growth factor on the cell cycle of cultured rabbit articular chondrocytes. *J Cell Physiol* 1990;143:534–545.
- Seyedin SM, Rosen DM, Segarini PR. Modulation of chondroblast phenotype by transforming growth factor-beta. *Pathol Immunopathol Res* 1988;7:38–42.
- Iwasaki M, Nakata K, Nakahara H, Nakase T, Kimura T, Kimata K, Caplan AI, Ono K. Transforming growth factor-beta 1 stimulates chondrogenesis and inhibits osteogenesis in high density culture of periosteum-derived cells. *Endocrinology* 1993;132:1603–1608.
- Majumdar MK, Banks V, Peluso DP, Morris EA. Isolation, characterization, and chondrogenic potential of human bone marrow-derived multipotential stromal cells. *J Cell Physiol* 2000;185:98–106.
- Morales TI. Transforming growth factor-beta 1 stimulates synthesis of proteoglycan aggregates in calf articular cartilage organ cultures. *Arch Biochem Biophys* 1991;286:99–106.
- Venn G, Lauder RM, Hardingham TE, Muir H. Effects of catabolic and anabolic cytokines on proteoglycan biosynthesis in young, old and osteoarthritic canine cartilage. *Biochem Soc Trans* 1990;18:973–974.
- van Beuningen HM, van der Kraan PM, Arntz OJ, van den Berg WB. Transforming growth factor-beta 1 stimulates articular chondrocyte proteoglycan synthesis and induces osteophyte formation in the murine knee joint. *Lab Invest* 1994;71:279–290.
- Hunziker EB, Driesang IM, Saager C. Structural barrier principle for growth factor-based articular cartilage repair. *Clin Orthop* 2001;S182–S189.
- Tabata Y, Hijikata S, Muniruzzaman M, Ikada Y. Neovascularization effect of biodegradable gelatin microspheres incorporating basic fibroblast growth factor. *J Biomater Sci Polym Ed* 1999;10:79–94.
- Hong L, Tabata Y, Miyamoto S, Yamada K, Aoyama I, Tamura M, Hashimoto N, Ikada Y. Promoted bone healing at a rabbit skull gap between autologous bone fragment and the surrounding intact bone with biodegradable microspheres containing transforming growth factor-beta1. *Tissue Eng* 2000;6:331–340.
- Hunziker EB, Driesang IM, Morris EA. Chondrogenesis in cartilage repair is induced by members of the transforming growth factor-beta superfamily. *Clin Orthop* 2001;S171–181.
- Jo S, Shin H, Shung AK, Fisher JP, Mikos AG. Synthesis and characterization of oligo(poly(ethylene glycol) fumarate) macromer. *Macromolecules* 2001;34:2839–2844.
- Temenoff JS, Park H, Jabbari E, Conway DE, Sheffield TL, Ambrose CG, Mikos AG. Thermally cross-linked oligo(poly(ethylene glycol) fumarate) hydrogels support osteogenic differentiation of encapsulated marrow stromal cells in vitro. *Biomacromolecules* 2004;5:5–10.
- Temenoff JS, Park H, Jabbari E, Sheffield TL, LeBaron RG, Ambrose C, Mikos AG. In vitro osteogenic differentiation of marrow stromal cells encapsulated in biodegradable hydrogels. *J Biomed Mater Res* 2004;70A:235–244.
- Holland TA, Tessmar J, Tabata Y, Mikos AG. Release of transforming growth factor-beta1 from gelatin microparticles en-

- capsulated in oligo(poly(ethylene glycol) fumarate) hydrogels in conditions that model the cartilage wound healing environment. *J Controlled Release* 2003;94:101–114.
34. Gao J, Dennis JE, Solchaga LA, Awadallah AS, Goldberg VM, Caplan AI. Tissue-engineered fabrication of an osteochondral composite graft using rat bone marrow-derived mesenchymal stem cells. *Tissue Eng* 2001;7:363–371.
 35. Solchaga LA, Yoo JU, Lundberg M, Dennis JE, Huibregtse BA, Goldberg VM, Caplan AI. Hyaluronan-based polymers in the treatment of osteochondral defects. *J Orthop Res* 2000;18:773–780.
 36. Solchaga LA, Gao J, Dennis JE, Awadallah A, Lundberg M, Caplan AI, Goldberg VM. Treatment of osteochondral defects with autologous bone marrow in a hyaluronan-based delivery vehicle. *Tissue Eng* 2002;8:333–347.
 37. Sheehan DC, Hrapchak BB. *Theory and practice of histotechnology*. Columbus, OH: Battelle Press; 1987.
 38. O'Driscoll SW, Keeley FW, Salter RB. The chondrogenic potential of free autogenous periosteal grafts for biological resurfacing of major full-thickness defects in joint surfaces under the influence of continuous passive motion. *J Bone Joint Surg Am* 1986;68:1017–1035.
 39. O'Driscoll SW, Keeley FW, Salter RB. Durability of regenerated articular cartilage produced by free autogenous periosteal grafts in major full-thickness defects in joint surfaces under the influence of continuous passive motion. A follow-up report at one year. *J Bone Joint Surg Am* 1988;70:595–606.
 40. Buma P, Pieper JS, van Tienen T, van Susante JL, van der Kraan PM, Veerkamp JH, van den Berg WB, Veth RP, van Kuppevelt TH. Cross-linked type I and type II collagenous matrices for the repair of full-thickness articular cartilage defects—A study in rabbits. *Biomaterials* 2003;24:3255–3263.
 41. Carranza-Bencano A, Garcia-Paino L, Armas Padron JR, Cayuela Dominguez A. Neochondrogenesis in repair of full-thickness articular cartilage defects using free autogenous periosteal grafts in the rabbit. A follow-up in six months. *Osteoarthritis Cartil* 2000;8:351–358.
 42. Agresti A. *Analysis of ordinal categorical data*. New York: John Wiley & Sons, Inc.; 1984.
 43. Stockwell RA. *Biology of cartilage cells*. New York: Cambridge University Press; 1979.
 44. Athanasiou KA, Korvick D, Schenck R. Biodegradable implants for the treatment of osteochondral defects in a goat model. *Tissue Eng* 1997;3:363–373.